neous ratio of the two signals at the extreme ends of the bandpass is examined. Variations in this ratio give a measure of the selective fading and are not influenced by nonselective fading. This ratio was analyzed in terms of its distribution over five-minute and one-hour periods. The most widely dispersed ratios observed during a one-hour period had a standard deviation estimated as 1.81 db. The average of the estimated standard deviations of the ratios within one-hour periods was 0.76 db. This again indicates adequate coherence across a 100-Mc modulation bandwidth. It is estimated that serious problems in transmitting information would arise if this standard deviation exceeds 3 db.

The actual correlation or signal ratio bandwidths may be somewhat better than the experiments indicate because of reading errors present in the method of analysis and because of the physical separation of the antennas for the two frequencies. Thus some degree of space diversity was present and influenced the results by reducing the correlation between the two signals and by increasing the dispersion in the ratios.

As a practical result, the measurements show that an adequate degree of coherence is obtainable during most of the time under the conditions of the experiment, except for short periods. Also, within-the-hour signal variations in the form of prolonged space-wave fadeouts are likely to occur, and have to be allowed for in systems design.

Note that these conclusions are based on measurements using two discrete frequencies at the ends of the 100-Mc band studied. There is no simple method for extending the results of these studies to a modulated signal occupying a 100-Mc frequency band, and it therefore seems desirable that tests be made using modulated signals over a path of this type before actual system development. It would also be desirable to extend the basic studies reported here to other climatic areas and other times of the year.

Acknowledgment

The studies reported here were made possible through the support of the U. S. Army Signal Research and Development Laboratories, who also supplied the X-band equipment used in the tests, and granted permission for the publication of this material. The measurements were performed by J. B. Snider and F. O. Guiraud of the Tropospheric Measurement Section, and the analysis done by personnel of the Propagation-Terrain Effects Section, both of the Radio Propagation Engineering Division of the Central Radio Propagation Laboratory; the digitizing of the magnetic tape data and related work was performed by personnel from the Data Reduction Instrumentation Section of the same Division.

The authors wish to thank K. A. Norton and H. B. Janes for their review and suggestions.

Curves for Ground Wave Propagation Over Mixed Land and Sea Paths*

J. R. WAIT†, FELLOW, IRE, AND L. C. WALTERS†, SENIOR MEMBER, IRE

Summary—**Specific numerical results are presented for ground wave propagation over paths which are part sea and part land. The problem is idealized to the extent that the earth is a smooth spherical surface. The method is based on a previous formulation in terms of mutual impedance between two vertical electric dipoles on an inhomogeneous spherical earth. Amplitude and phase of the ground wave are given for various combinations of the following parameters: frequency 1000, 100, and 20 kc; land conductivities 100 and 10 mmhos/meter; and a sea conductivity of 4 mhos/meter. Most of the curves exhibit the well-known recovery effect which occurs beyond the coast line for propagation from land towards the sea.**

Introduction

IT IS THE PRIME purpose of this paper to illustrate graphically the propagation of vertically polarized ground waves over a spherical earth across boundaries separating contrasting media. Although the theoretical problem has been discussed extensively in the literature [1]–[3] very little factual information is available for the use of radio engineers. The situation is particularly acute at low frequencies where some of the series solutions are not of sufficient accuracy or they have very poor convergence.

The problem is illustrated in Fig. 1 where a vertical cross section of the earth is shown. As indicated, two vertical dipoles at A and B are located on a spherical earth of radius a. The other symbols have the following meaning: d is the (great circle) distance measured along

* Received May 9, 1962. This paper was presented at a meeting of the International Scientific Radio Union, Washington, D. C., May 2, 1962. The research reported here was supported in part by the Advanced Research Projects Agency under Contract Order No. 183-62 and A.F. Cambridge Research Laboratories under Contract PRO-61-568.

† Central Radio Propagation Laboratory, National Bureau of Standards, Boulder, Colo.

the surface of the earth between A and B; the lengths of the two portions of the path are d_1 and d_2; the medium to the left of the boundary has conductivity σ and dielectric constant ϵ; the medium to the right of the boundary has conductivity σ_1 and dielectric constant ϵ_1; and finally α is the distance from B to a variable point P on d_1.

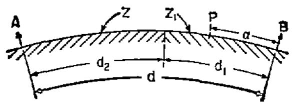

Fig. 1—Two-section path on a spherical earth. The boundary of separation is here taken to be perpendicular to the path AB.

For $\alpha > d_1$, the surface impedance is

$$Z \cong \left[\frac{i\mu_0\omega}{\sigma + i\epsilon\omega}\right]^{1/2}\left[1 - \frac{i\epsilon_0\omega}{\sigma + i\epsilon\omega}\right]^{1/2}, \tag{1}$$

while for $\alpha < d_1$

$$Z_1 \cong \left[\frac{i\mu_0\omega}{\sigma_1 + i\epsilon_1\omega}\right]^{1/2}\left[1 - \frac{i\epsilon_0\omega}{\sigma_1 + i\epsilon_1\omega}\right]^{1/2}, \tag{2}$$

where μ_0 is the permeability of the whole space, assumed constant, and ϵ_0 is the permittivity of free space. (In mks units $\mu_0 = 4\pi \times 10^{-7}$ and $\epsilon_0 = 8.854 \times 10^{-12}$.) The fields vary according to exp $(+i\omega\tau)$ when ω is the angular frequency and τ is time.

The basic problem is to compute the mutual impedance between the dipoles A and B for the mixed path described. This complex quantity is denoted Z_{ab}'. If the path were homogeneous the impedance is denoted Z_{ab} which is well known.

Method of Solution

To within a very good approximation, the mutual impedance can be expressed as a one-dimensional integral with limits from $\alpha = 0$ to d_1 along the great circle path [4]. This integral is expressed in terms of certain attenuation functions $W(d, z)$ and $W(d, Z, Z')$ defined by the following relationships:

$$Z_{ab} = \frac{l_a l_b i\mu_0\omega}{2\pi d} e^{-ikd} W(d, Z)\left(1 + \frac{1}{ikd} - \frac{1}{k^2d^2}\right) \tag{3}$$

$$Z_{ab}' = \frac{l_a l_b i\mu_0\omega}{2\pi d} e^{-ikd} W(d, Z, Z_1)\left(1 + \frac{1}{ikd} - \frac{1}{k^2d^2}\right) \tag{4}$$

where l_a and l_b are the effective lengths of the dipoles A and B. The W functions are normalized to approach 1 if the earth were flat and perfectly conducting. Thus, under the further restriction that $d \ll a$, [5], $W(d, Z, Z_1) \cong W(d, Z)$ for $d_1 < 0$, and

$$W(d, Z, Z_1) \cong W(d, Z) - \left(\frac{ikd}{2\pi}\right)^{1/2} \frac{(Z_1 - Z)}{\eta_0} \int_0^{d_1} \frac{W(d-\alpha, Z)W(\alpha, Z_1, Z)}{[\alpha(d-\alpha)]^{1/2}} d\alpha \tag{5}$$

for $d_1 > 0$, where $\eta_0 = (\mu_0/\epsilon_0)^{1/2} \cong 120\pi$. Since $\alpha < d_1$ over the range of integration, $W(\alpha, Z_1, Z)$ in the integrand may be replaced by $W(\alpha, Z_1)$ as follows:

$$W(d, Z, Z_1) \cong W(d, Z) - \left(\frac{ikd}{2\pi}\right)^{1/2} \frac{(Z_1 - Z)}{\eta_0} \int_0^{d_1} \frac{W(d-\alpha, Z)W(\alpha, Z_1)}{[\alpha(d-\alpha)]^{1/2}} d\alpha. \tag{6}$$

As (5) and (6) express the attenuation function over an inhomogeneous earth, in terms of the attenuation function over a homogeneous earth it is necessary to compute the latter. The computational methods for this are well known from the work of van der Pol and Bremmer [6] and Fock [7]. Thus

$$W(d, Z) = \left(\frac{\pi x}{i}\right)^{1/2} \sum_{s=1,2,3,\cdots}^{\infty} \frac{e^{-ixt_s}}{t_s - q^2} \tag{7}$$

where

$$x = \left(\frac{ka}{2}\right)^{1/2}\left(\frac{d}{a}\right), \quad \text{and} \quad iq = \left(\frac{ka}{2}\right)^{1/3}\left(\frac{Z}{\eta_0}\right).$$

The coefficients t_s are roots of

$$w'(t) - qw(t) = 0 \tag{8}$$

where $w(t)$ is an Airy integral and the prime indicates a derivative with respect to t. In terms of Hankel functions of order one-third,

$$w(t) = \left[\exp\left(-\frac{2\pi i}{3}\right)\right]\left(-\frac{\pi t}{3}\right)^{1/2} H_{1/3}^{(2)}[(2/3)(-t)^{3/2}].$$

This notation is similar to that used by Fock [7]. Series such as these given by (7) have been programmed for a computer recently by a number of investigators [8]–[10].

The above series, known as the residue series, converges slowly for short distances and low frequencies. In these instances, a modified flat earth series was used [11], [2].

$$W(d, Z) = \sum_{m=0,1,2,\cdots} A_m e^{im\pi/4} q^m (x)^{m/2} \tag{9}$$

where

$$A_0 = 1, \qquad A_1 = -i\sqrt{\pi},$$

$$A_2 = -2, \qquad A_3 = i\sqrt{\pi}\left(1 + \frac{1}{4q^3}\right),$$

$$A_4 = \frac{4}{3}\left(1 + \frac{1}{2q^3}\right), \qquad A_5 = -\frac{i\sqrt{\pi}}{2}\left(1 + \frac{3}{4q^3}\right),$$

$$A_5 = -\frac{8}{15}\left(1 + \frac{1}{q^3} + \frac{7}{32q^6}\right), \text{ etc.}$$

By use of (7) or (9), whichever is appropriate, the W functions for homogeneous paths occurring in (6) can be computed. Some preliminary results using such an approach have already been reported [5], [12].

With successive applications of the techniques to evaluate W for a two-part medium, it is possible to extend the theory to a three-part medium [2]. The path between A and B consists of three segments d_3 with surface impedance Z, d_2 with surface impedance Z_2, and d_1 with surface impedance Z_1 (see Fig. 2).

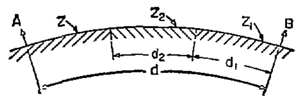

Fig. 2—Three-section path on a spherical earth. Both boundaries of separation are taken to be perpendicular to the path AB.

$$
\begin{aligned}
W(d, Z, Z_2, Z_1) &= W(d, Z) \\
&- \left(\frac{ikd}{2\pi}\right)^{1/2} \frac{Z_1 - Z}{\eta_0} \int_0^{d_1} \frac{W(d-\alpha, Z) W(\alpha, Z_1)}{[\alpha(d-\alpha)]^{1/2}} d\alpha \\
&- \left(\frac{ikd}{2\pi}\right)^{1/2} \frac{Z_2 - Z}{\eta_0} \int_{d_1}^{d_1+d_2} \frac{W(d-\alpha, Z) W(\alpha, Z_1, Z_2)}{[\alpha(d-\alpha)]^{1/2}} d\alpha
\end{aligned}
\tag{10}
$$

where $W(d, Z)$ is the attenuation function for propagation from A to B over a homogeneous earth of surface impedance Z. $W(d-a, Z)$ and $W(\alpha, Z_1)$ are attenuation functions for propagation over homogeneous surfaces of surface impedances Z and Z_1, respectively. $W(\alpha, Z_1, Z_2)$ is the two-section attenuation function for propagation from B to a point α on d_2. It follows readily from (6) that

$$
\begin{aligned}
W(\alpha, Z_1, Z_2) &= W(\alpha, Z_1) \\
&- \left(\frac{ik\alpha}{2\pi}\right)^{1/2} \frac{Z_2 - Z_1}{\eta_0} \int_0^{\alpha-d_1} \frac{W(\alpha-\alpha', Z_1) W(\alpha', Z_2)}{[\alpha'(\alpha-\alpha')]^{1/2}} d\alpha'.
\end{aligned}
\tag{11}
$$

It should be pointed out that these convolution integrals can be evaluated in terms of doubly infinite series if the residues series representations for the W functions in the integrand are employed. This approach has been discussed before [3], [5]. It leads to results which are identical to those derived by Furutsu [13] using an entirely different method. Unfortunately, such doubly infinite series are very poorly convergent at low frequencies, although they are very suitable for higher frequencies.

Outline of Numerical Methods Used

The convolution integrals in [5], [10], and [11] were evaluated in an efficient manner by Gaussian quadrature [14] in conjunction with a high-speed computer. A short description of the method is given.

In quadrature methods a definite integral of a function is approximated by a weighted sum of particular values of the ordinate with the abscissas properly distributed in the limits of integration. Thus,

$$
\int_a^b f(x) dx = \sum_{j=1}^{n} H_j f(a_j) + E_n. \tag{12}
$$

The abscissas a_j are roots of the Legendre polynomials, the weights H_j are functions of these roots, and E_n is the error term which can, in general, be made arbitrarily small with increasing n. The Gaussian roots and weights are tabulated for various n for limits between -1 and 1 [15], but other limits can be used by a change of variable as follows:

$$
\int_a^b f(x) dx = \frac{b-a}{2} \int_{-1}^{1} g(y) dy
$$

where

$$
x = \frac{b-a}{2} y + \frac{b+a}{2}. \tag{13}
$$

Furthermore, in the Gaussian quadrature procedure, the integrand is approximated by a polynomial of $(2n-1)$ degree which has the same ordinates as the function for n discrete abscissas.

To evaluate the attenuation functions in (5), (10), and (11) by the method described above, a table of these functions for abscissas at arbitrary intervals was evaluated for a given frequency, conductivity, and dielectric constant using (7) and (9), whichever was appropriate. The attenuation W for a particular Gaussian abscissa was then found by Lagrangian interpolation [14]. In this method, since the values of the function $f(x)$ were available for $(n+1)$ discrete values of the abscissas $a_0, a_1, a_2, \cdots, a_n$, a power polynomial of degree n coinciding at $x = a_0, a_1, \cdots, a_n$ with given values of $f(a_j)$ was constructed. Then the value of $f(x)$ for this polynomial for any desired Gaussian x was expressed, in terms of given abscissas with corresponding $f(a_j)$, as follows:

$$
f(x) = \sum_{j=0}^{n} \frac{(x-a_0)(x-a_1)\cdots(x-a_{j-1})(x-a_{j+1})\cdots(x-a_n) f(a_j)}{(a_j-a_0)(a_j-a_1)\cdots(a_j-a_{j-1})(a_j-a_{j+1})\cdots(a_j-a_n)}. \tag{14}
$$

Eq. (14) is actually the Lagrange interpolation formula which expresses $f(x)$ as a weighted mean of the given ordinates with weights which are functions of the abscissas, referred to as the Lagrangian interpolation coefficients. Eq. (14) was used for interpolation ($a_0 < x < a_n$) or extrapolation $x > a_n$ or $x < a_0$ for any value of the argument.

With the procedure described above, the actual calculations of the attenuation functions for mixed paths were carried out on a high-speed digital computer (CDC 1604). The program was first written to calculate W, the attenuation factor, for a given frequency, conductivity, and dielectric constant for an arbitrarily spaced number of distances for a homogeneous path. The output of this program was a number of tables using various combinations of frequency, conductivity, and dielectric constant with varying distance which were used repeatedly for different variations of path as input for the second program.

The purpose of the second program was to calculate the attenuation function for a two-part mixed path. With the W's available at certain distances for each part of the path from the first program, the W's necessary for Gaussian distances were found by Lagrange interpolation. The convolution integrals are then quickly and easily evaluated by Gaussian quadrature and the attenuation function W for the two-part mixed path completed.

Using essentially the same techniques, the W's for the three-part path were also calculated for a limited number of cases. In principle, the method can be applied to a path with any number of segments.

Discussion of Results

It is obvious that any attempt to present curves and tables which completely cover all cases of practical interest is futile. The large number of parameters involved quickly lead us to an enormous number of curves. However, with some care it is possible to limit these to several hundred curves if the user is asked to interpolate to some extent. It is hoped to publish such an atlas of curves in the future. In the meantime, it is considered worthwhile to present a sampling of those results in graphical form.

For the most part, the cases shown in the following figures are for propagation over a two-part path consisting of homogeneous sea and land portions [Figs. 3(a)–8, pages 42–44]. One example of a three-part path is also shown (Fig. 9). The electrical constants for the land were taken as $\sigma=10^{-2}$ mhos/m and $\epsilon/\epsilon_0=15$ corresponding to well-conducting land, and $\sigma=10^{-3}$ mhos/m and $\epsilon/\epsilon_0=15$ corresponding to poorly conducting land. For sea water $\sigma=4$ mhos/m and $\epsilon/\epsilon_0=80$. To allow for standard atmospheric refraction, the effective radius concept was utilized [16]. For the results shown here, a was set equal to four-thirds times the actual radius.

In each case the amplitude of $W(d, Z, Z_1)$ and the phase lag (*i.e.*, $-\arg W$) are plotted as a function of distance d in kilometers. For these calculations the heights of the antennas above ground are assumed to be zero. The frequencies chosen are 1000, 100, and 20 kc. The length of the second section d_2 is indicated on each curve.

The preceding formulation was in terms of mutual impedance between vertical dipoles A and B. For further discussion it is probably better to express the results in terms of the vertical electric field at B for a standard source at A. For example,

$$E = E_0W = E_0\left|W\right|e^{-i\Phi}$$

where $|W|$ is the amplitude of the relative field, Φ is the phase lag, and

$$E_0 = \frac{100}{d}\left[1 - \frac{1}{(kd)^2} - \frac{i}{kd}\right]e^{-ikd}\text{ volts/m.}$$

For a flat perfectly conducting plane E would be equal to the field E_0. The strength of the source is thus chosen so that the radiation field is 0.1 volt/m at $d=1$ km. In most cases of practical interest, $kd\gg1$ and

$$E_0 \cong (100/d)e^{-ikd}.$$

Thus, in the far field, W is proportional to the actual field times distance. Speaking loosely, W can be described as the actual field divided by the "inverse-distance" field.

It should be kept in mind that at short distances, where d is comparable with or less than a wavelength, the terms corresponding to $1/(ikd)$ and $1/(ikd)^2$ in (4) should be retained. These correspond to what are often called the induction and static fields, respectively. It is also worth mentioning that if the receiving antenna (at B) was a vertical loop, the horizontal magnetic field component H would be measured. Thus

$$H = H_0W$$

where

$$\eta_0H_0 = \frac{100}{d}\left[1 - \frac{i}{kd}\right]e^{-ikd}$$

is also expressed in volts/meter if $\eta_0=120\pi$ ohms. Again, on a flat perfectly conducting earth $\eta_0H_0=0.1$ volt/m at $d=1$ km, provided $kd\gg1$. In this case there is no static field component.

There are many other situations in which the W functions enter into the field formulas. In general, they characterize the vertical polarized component of any physical source placed on or near the earth's surface. Furthermore, the source or receiver may be buried in the ground or submerged in the sea.

Some specific features of the curves are now worth discussing. In this portion, the W functions will be referred to as the "relative field."

In Fig. 3(a), for 1000 kc, the path of propagation is from land to sea. It is apparent that the relative field increases beyond the coast line in each case. For the greater distances the effect is very marked. Such a phenomenon has been observed experimentally by Millington [17] and has been called the recovery effect. The corresponding phase curves are shown in Fig. 3(b). The rather abrupt drop in the phase lag just beyond the coast line could be called a phase recovery. Such an effect has been confirmed experimentally by Pressey, Ashwell, and Fowler [18].

An additional set of land-to-sea curves for 1000 kc are given in Figs. 4(a) and 4(b). Here, the relatively poor conductivity of the land (*i.e.*, 10^{-3}) leads to very marked recovery effects beyond the coast line. The

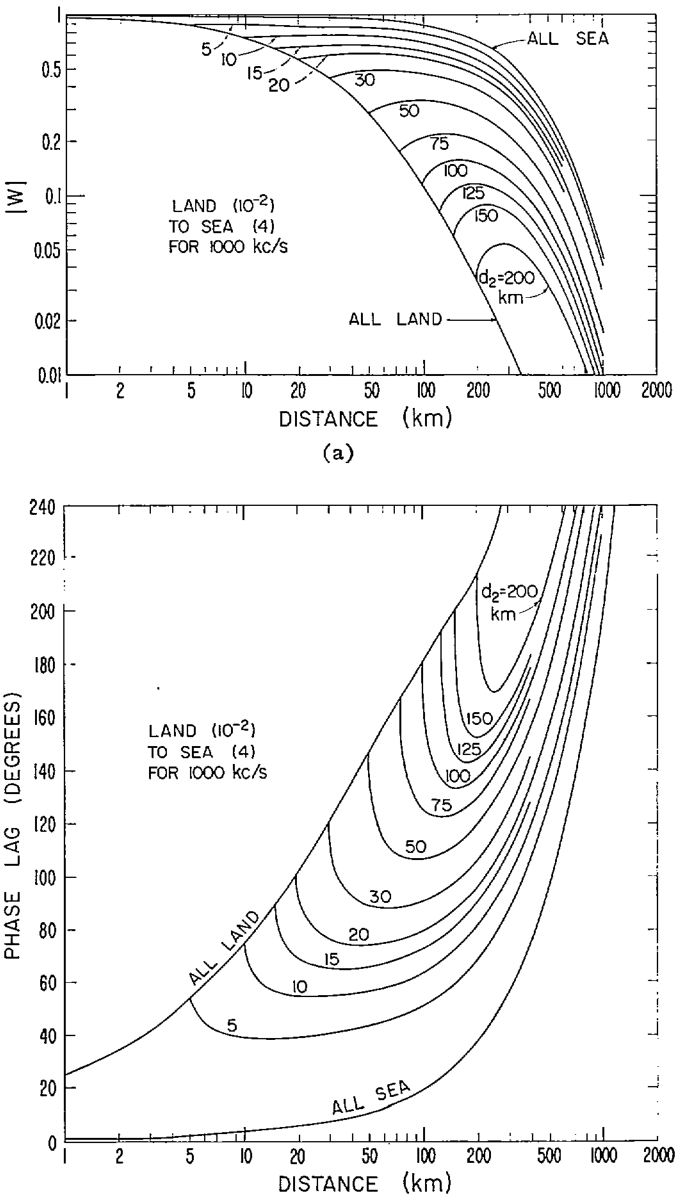

Fig. 3—(a) Amplitude of the relative field of the ground wave as a function of distance for propagation from land towards the sea. The coast line is a distance d_2 from the transmitter (which is on the land). (b) Phase of the relative field corresponding to conditions of Fig. 3(a).

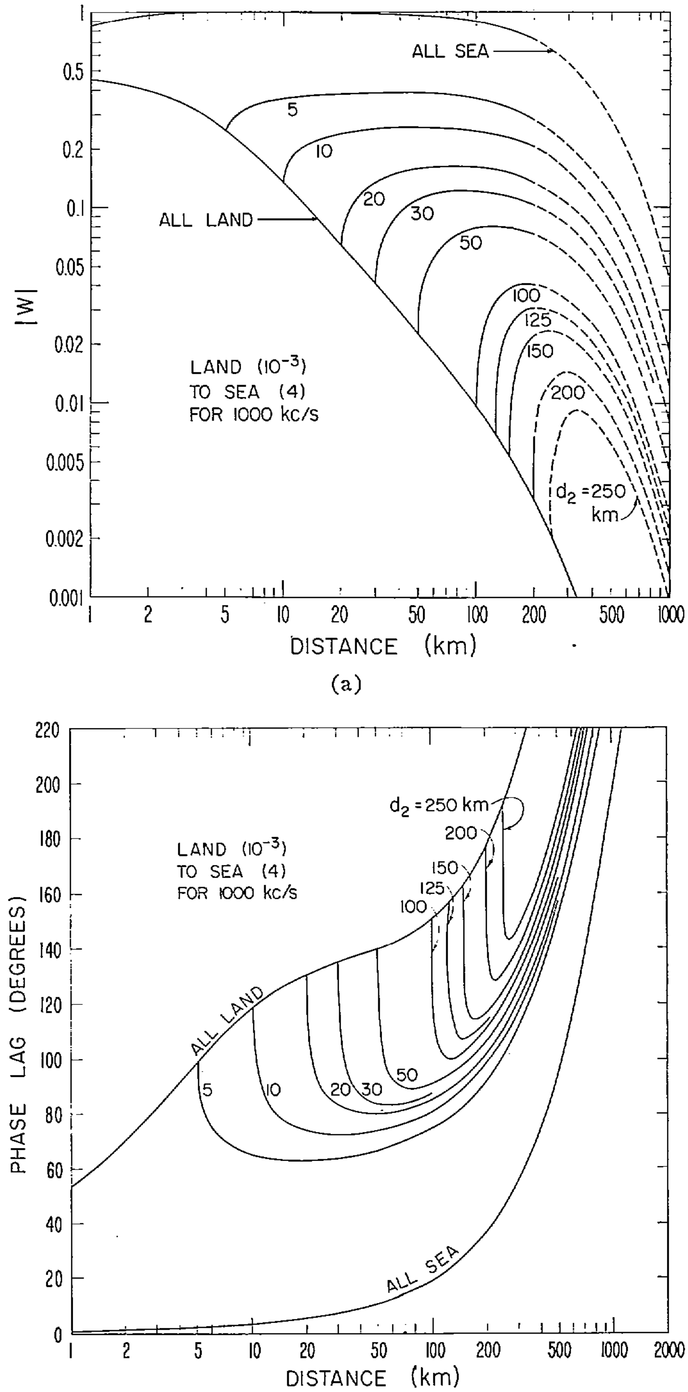

Fig. 4—(a) Amplitude of the relative field of the ground wave as a function of distance for propagation from land towards the sea. The coast line is a distance d_2 from the transmitter (which is on land). (b) Phase of the relative field corresponding to conditions of Fig. 4(a).

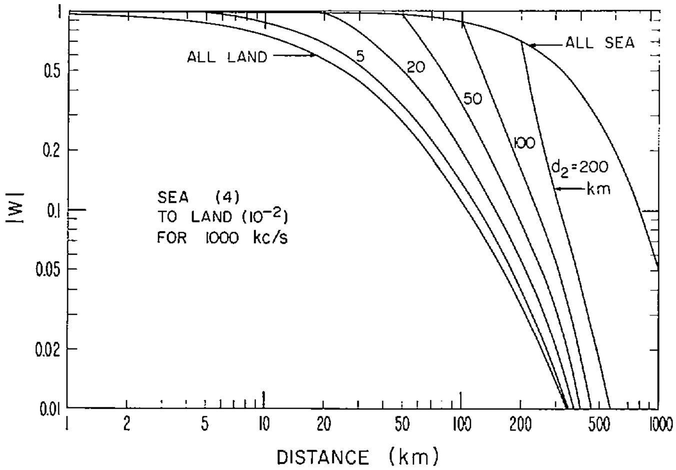

Fig. 5—Amplitude of the relative field of the ground wave as a function of distance for propagation from sea towards the land. The coast line is a distance d_2 from the transmitter.

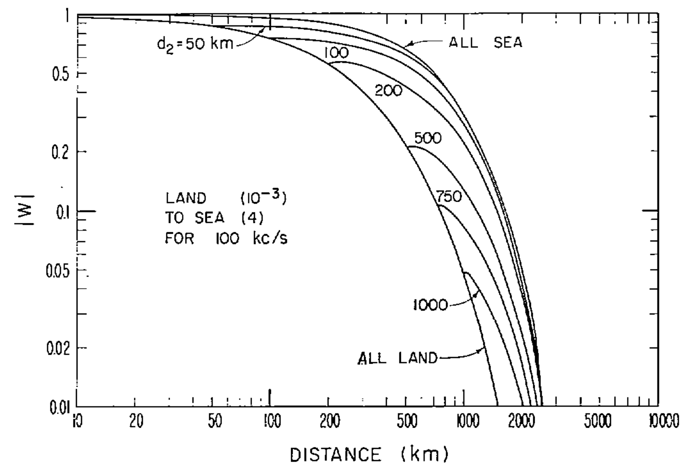

(a)

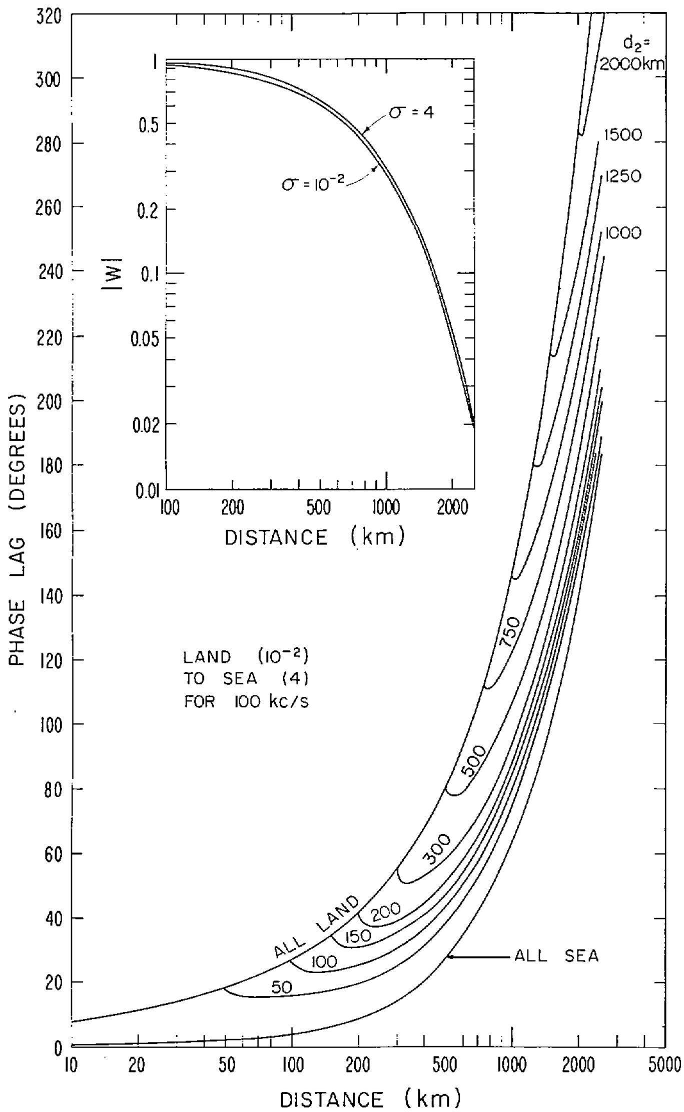

Fig. 6—Amplitude and phase of the relative field as a function of distance for propagation from land to sea.

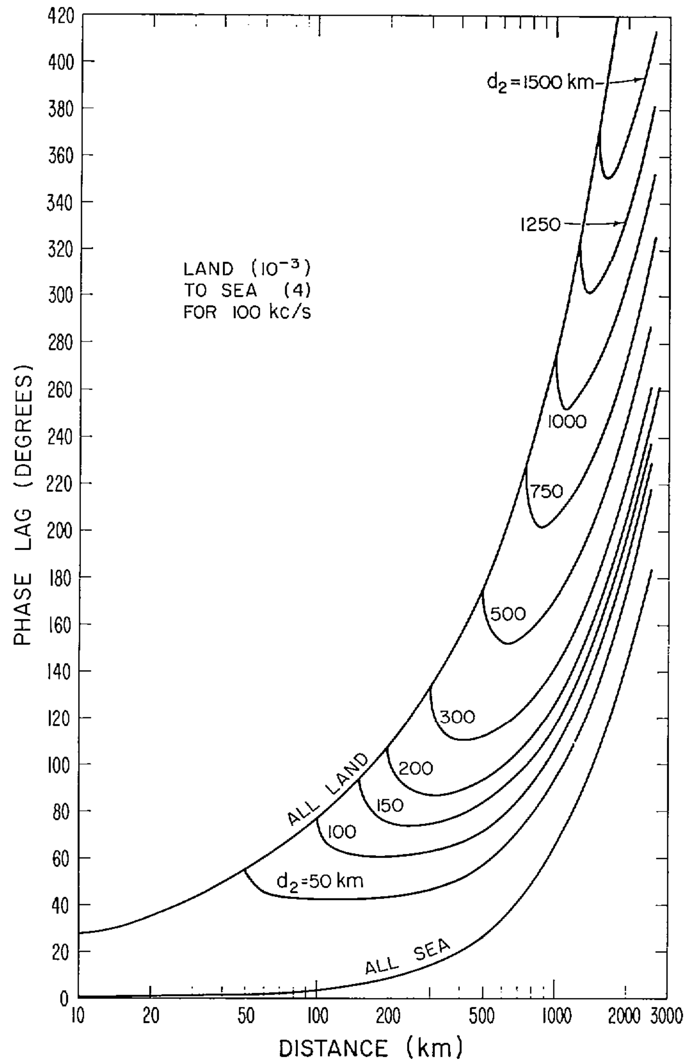

(b)

Fig. 7—(a) Amplitude of the relative field of the ground wave as a function of distance for propagation from land towards the sea. The coast line is a distance d_2 from the transmitter (which is on land). (b) Phase of the relative field corresponding to conditions of Fig. 7(a).

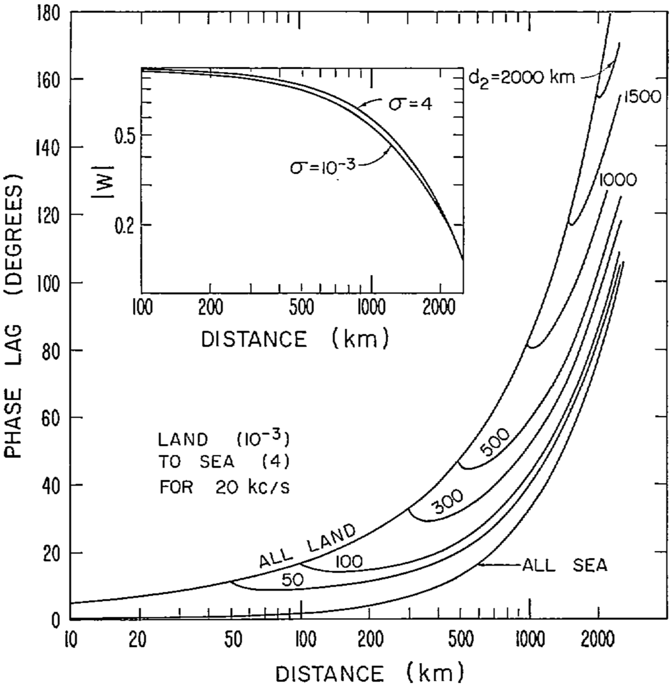

Fig. 8—Amplitude and phase of the relative field as a function of distance for propagation from land to sea.

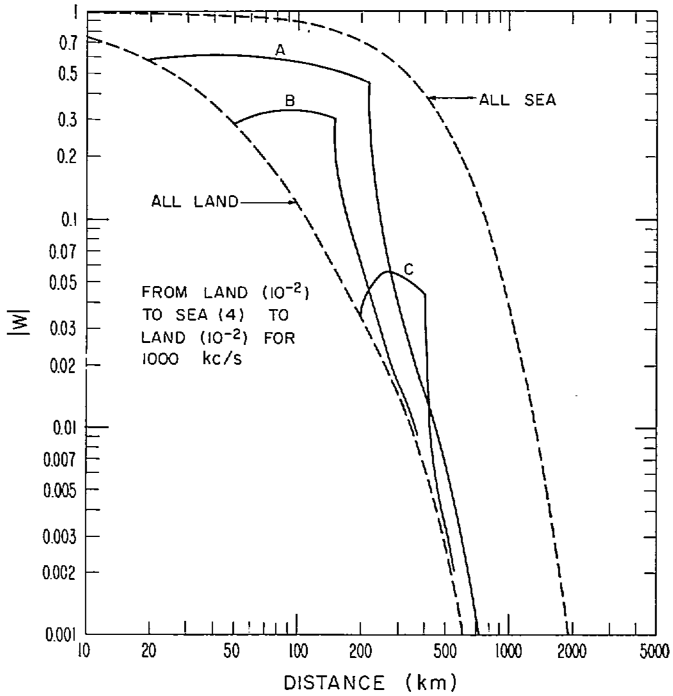

Fig. 9—Amplitude of the relative field for propagation over a three-section path consisting of two land portions separated by a sea portion.

right-hand portion of the amplitude curves in Fig. 4(a) are shown dashed to emphasize that under these conditions the ionospheric reflected waves may overwhelm the ground wave. However, in certain pulsed-type transmissions such as used in Loran, the ground wave may be observed separately from the sky waves even at very great ranges. Nevertheless, it is well to keep in mind that ionospheric influences are not considered in these curves.

Ground wave propagation at 1000 kc from sea to land is illustrated in Fig. 5 where the amplitude of the relative field is plotted as a function of distance. In this case, the transmitter is located over the sea. Here, as expected, the field drops abruptly as the coast line is crossed. Actually, there is no new information in Fig. 5 that was not in Fig. 3(a) since, by reciprocity, the transmitter and receiver locations can always be exchanged. Consequently, it would be somewhat redundant to show the phase curves.

At lower frequencies the phenomena described above also occur. However, as indicated in Fig. 6 for 100 kc and a land conductivity of 10^{-2}, the recovery phenomenon is not so marked. In fact, for the amplitude of the field there is hardly any difference between an all-land path and an all-sea path. This is consistent with the well-known fact that the characteristics of ground wave propagation at low frequencies are determined mainly by the curvature of the earth rather than its electrical properties. However, for poorer ground conductivity, the recovery effects even at 100 kc, are significant. Examples of these are shown in Figs. 7(a) and 7(b) for a land conductivity of 10^{-3}.

Ground wave propagation from land to sea at very low frequencies is illustrated in Fig. 8 for a land conductivity of 10^{-3}. Here, even though a poor land conductivity has been chosen, the recovery effects are not marked.

Finally, in Fig. 9 an example of a three-part path is shown. The propagation, for 1000 kc, is from land to sea to land. In each case it is noted that a recovery effect takes place as the first coast line is crossed. Then, at the second coast line the field drops abruptly. In each of the three cases shown the amplitude curves, asymptotically, at large distances, approach the curve for an all-land path. However, in each case there is residual vertical displacement which is approximately proportional to the length of the intermediate sea-portion of the path. This phenomenon was discussed previously [4].

Concluding Remarks

The curves presented in this paper are all based on the assumption that the heights of the transmitting and receiving antennas are effectively zero. Without additional computation it is not possible to say much about the height variation of the fields over mixed paths. However, it is to be expected that the recovery effects are less marked as the receiving antenna is raised. In fact, this is necessary from a physical basis since energy must be supplied from greater heights if the field is actually to increase with distance on the earth's surface. This is confirmed by an examination of the structure of the general formula for arbitrary heights [4]. Such a mechanism was also suggested by Millington [17].

Most of the complications in the height gain function would occur at or just near the coast lines. Somewhat beyond the coast line the situation becomes much simpler. For example, on examining any of the curves in Figs. 3(a)–8 it is noted that the field variations with distance always approach that expected for a homogeneous medium. This is also observed in the structure of the theoretical forms [4]. Consequently, in these limiting cases it may be asserted that the height gain functions are characteristic only of the underlying medium. In fact, for low heights

$$\frac{E \text{ (at height } z)}{E \text{ (at height } 0)} \cong 1 + ikz(Z/\eta_0)$$

where Z is the surface impedance of the underlying earth's surface, $\eta_0 = 120\pi$, and $k = 2\pi/\text{wavelength}$. This simple formula is valid provided $(ka)^{-2/3}(kz)^2 \ll 1$ [19]; also, as mentioned, it must only be used sufficiently far from the coast line.

Some of the important features of the characteristics of mixed-path propagation have been observed experimentally as mentioned above. While the observed effects are consistent with theory, it is difficult to find conditions which are suitably idealized. For example, the land portions of the path are usually inhomogeneous and not sufficiently smooth. A much better way experimentally to confirm theory is to set up a model experiment. With this motivation an extensive laboratory investigation of mixed-path propagation has been initiated. Some of the first results [20] obtained in this study indicate very satisfactory agreement with theory.

Acknowledgment

The author would like to thank Mrs. F. Whelan for her assistance in drafting the illustrations and Mrs. E. Brackett for her help in preparing the manuscript.

References

[1] J. R. Wait, "Mixed-path ground wave propagation, I. Short distances," *J. Res. NBS*, vol. 57, pp. 1–15; July, 1956.

[2] J. R. Wait, "On the theory of propagation of electromagnetic waves along a curved surface," *Canad. J. Phys.*, vol. 36, pp. 9–17; January, 1958.

[3] E. L. Feinberg, "Propagation of radio waves along an inhomogeneous surface," *Nuevo Cim.*, vol. 11 (suppl.), ser. 10, pp. 60–91; January, 1959. (This paper contains an extensive bibliography of Russian papers on the subject.)

[4] J. R. Wait, "On the theory of mixed-path ground-wave propagation on a spherical earth," *J. Res. NBS*, vol. 65D, no. 4, pp. 401–410; July–August, 1961.

[5] J. R. Wait and J. Householder, "Mixed-path ground propagation, 2. Larger distances," *J. Res. NBS*, vol. 59, no. 1, pp. 19–26; July, 1957.

[6] B. van der Pol and H. Bremmer, "The diffraction of electromagnetic waves from an electrical point source round a finitely conducting sphere," *Phil. Mag.*, vol. 24, ser. 7, pp. 141–176; July, 1937.

[7] V. A. Fock, "Diffraction of radio waves around the earth's surface," *J. Phys. USSR*, vol. 9, pp. 256–266, April, 1945; and *J. Theo. Exp. Phys.*, vol. 15, pp. 480–490, June, 1945.

[8] J. R. Wait and H. H. Howe, "Amplitude and Phase Curves for Ground Wave Propagation in the Band 200 c/s to 500 kc/s," Natl. Bur. Standards, Washington, D. C., NBS Circular No. 574; May, 1956.

[9] J. R. Johler, L. C. Walters, and C. M. Lilley, "Amplitude and Phase of the Low- and Very-Low Radio Frequency Ground Wave," Natl. Bur. Standards, Washington, D. C., NBS Tech. Note No. 60 (PB 161561); June 1, 1960.

[10] I. H. Gerks, private communication, 1962.

[11] H. Bremmer, "Applications of operational calculus to ground wave propagation, particularly for long waves," IRE Trans. on Antennas and Propagation, vol. AP-6, pp. 267–272; July, 1958.

[12] J. R. Johler and C. M. Lilley, "Evaluation of Convolution Integrals Occurring in the Theory of Mixed Path Propagation," Natl. Bur. Standards, Washington, D. C., NBS Tech. Note No. 132 (PB 161633); October 15, 1961.

[13] K. Furutsu, "Propagation of electromagnetic waves over a flat earth across two boundaries separating three different media," *J. Radio Res. Labs.* (*Tokyo*), vol. 2, pp. 239–279, July, 1955; and "Propagation of electromagnetic waves over the spherical earth across boundaries separating different earth media," vol. 2, pp. 345–398, October, 1955.

[14] F. Kopal, "Numerical Analysis," John Wiley and Sons, Inc., New York, N. Y.; 1955.

[15] P. Davis and P. Rabinowitz, "Abscissas and weights for Gaussian quadratures of high order," *J. Res. NBS*, vol. 56, pp. 35–37; January, 1956.

[16] K. A. Norton, "The calculation of the ground wave field intensity over a finitely conducting spherical earth," Proc. IRE, vol. 29, pp. 623–639; December, 1941.

[17] G. Millington, "Ground wave propagation over an inhomogeneous smooth earth, I," *Proc. IEE*, vol. 96, p. 53; January, 1949. See also *Nature*, vol. 163, p. 128; 1949 and vol. 164, p. 114; 1949.

[18] B. G. Pressey, G. E. Ashwell, and C. S. Fowler, "Change of phase of a low-frequency ground wave propagated across a coast line," *Proc. IEE*, vol. 103B, p. 527; July, 1956.

[19] J. R. Wait, "Radiation from a vertical antenna over a curved stratified ground," *J. Res. NBS*, vol. 56, No. 4, pp. 237–244; April, 1956.

[20] S. W. Maley, private communication, 1962.